

Evolutionary paths among different red galaxy types at $0.3 < z < 1.5$ and the buildup of massive E-S0's

Jesús Gallego, Mercedes Prieto, M.Carmen Eliche-Moral, Marc Balcells, David Cristóbal-Hornillos, Peter Erwin, David Abreu, Lilian Domínguez-Palmero, Angela Hempel, Carlos López-Sanjuan, Rafael Guzmán, Pablo G. Pérez González, Guillermo Barro and Jaime Zamorano

GOYA project collaboration



ULL

Universidad de La Laguna



INTRODUCCION

Mass downsizing seems to conflict with hierarchical models of galaxy formation about the epoch of definitive buildup of massive E-S0's and the role played by major mergers in it. We re-address this question by analysing the morphology, structural distortion level, and star formation enhancement of a sample of massive galaxies ($M_* > 5 \times 10^{10} M_\odot$) lying on the Red Sequence and its surroundings (green valley) at $0.3 < z < 1.5$. We have used an initial sample of ~ 1800 sources with $K_s < 20.5$ mag over an area ~ 155 arcmin² on the Groth Strip, combining broad-band multi-wavelength data from the Rainbow Extragalactic Database and the GOYA Survey.

ANALYSIS

1 Red galaxies selection

Apparent color cuts have been used to separate red from blue galaxies. The figure shows the bimodal distribution of these galaxies up to $z \sim 2$.

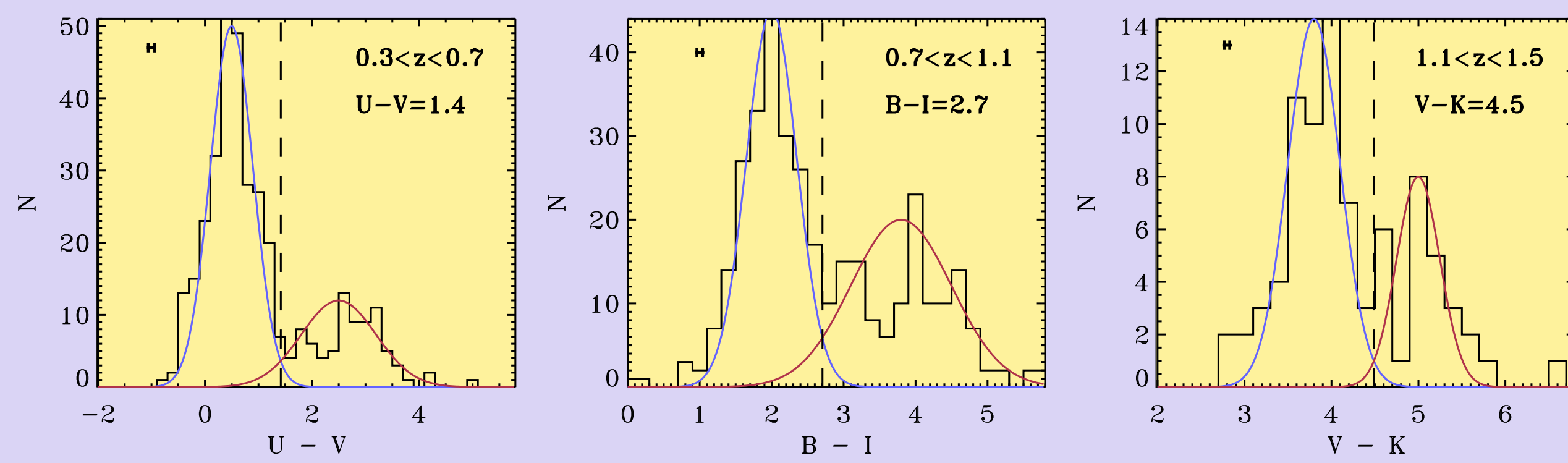


Figura 1.- Color histograms of all galaxies in the K-band selected catalogue in the three wide redshift bins under consideration. The apparent color are the nearest to the rest-frame U-B at each redshift interval. Red and blue solid lines: Gaussian functions fitted to match the bimodal color distributions at each redshift. Vertical dashed lines: Color cuts used to isolate red from blue galaxies in each redshift bin.

2 Visual morphological and structural classification

2 Visual morphological and structural classification

The following morphological and structural types of red galaxies have been defined: Compacts (C), RegularSpheroid (RS), Regular Disk (RD), Irregular Spheroid (IS), Irregular Disk (ID).

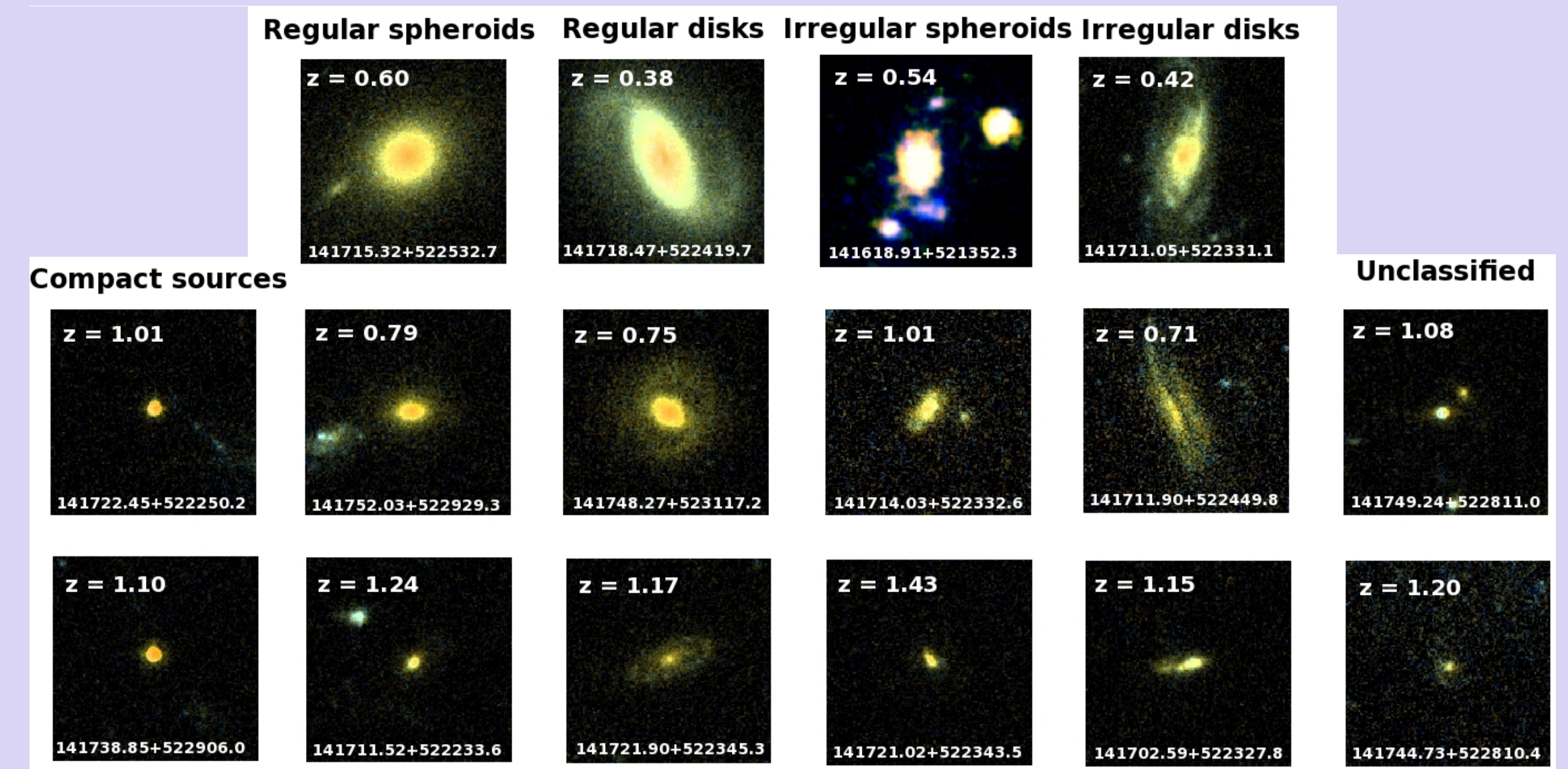


Figura 2.- False-color postage stamps of some red galaxies in our sample, obtained using the V and I bands. One example representative of each type is shown for each wide redshift bin used in the present study ($0.3 < z < 0.7$, $0.7 < z < 1.1$, and $1.1 < z < 1.5$). North is up, East is left. The frames correspond to a $5'' \times 5''$ field-of-view, except for the irregular spheroid 141618.91+521352.3, where a $10'' \times 10''$ view is used.

3 Classification according to star formation activity

SFR cuts have been used to define the red galaxies with enhanced SFRs compared to the average SFR of the galaxy population, as a function of redshift.

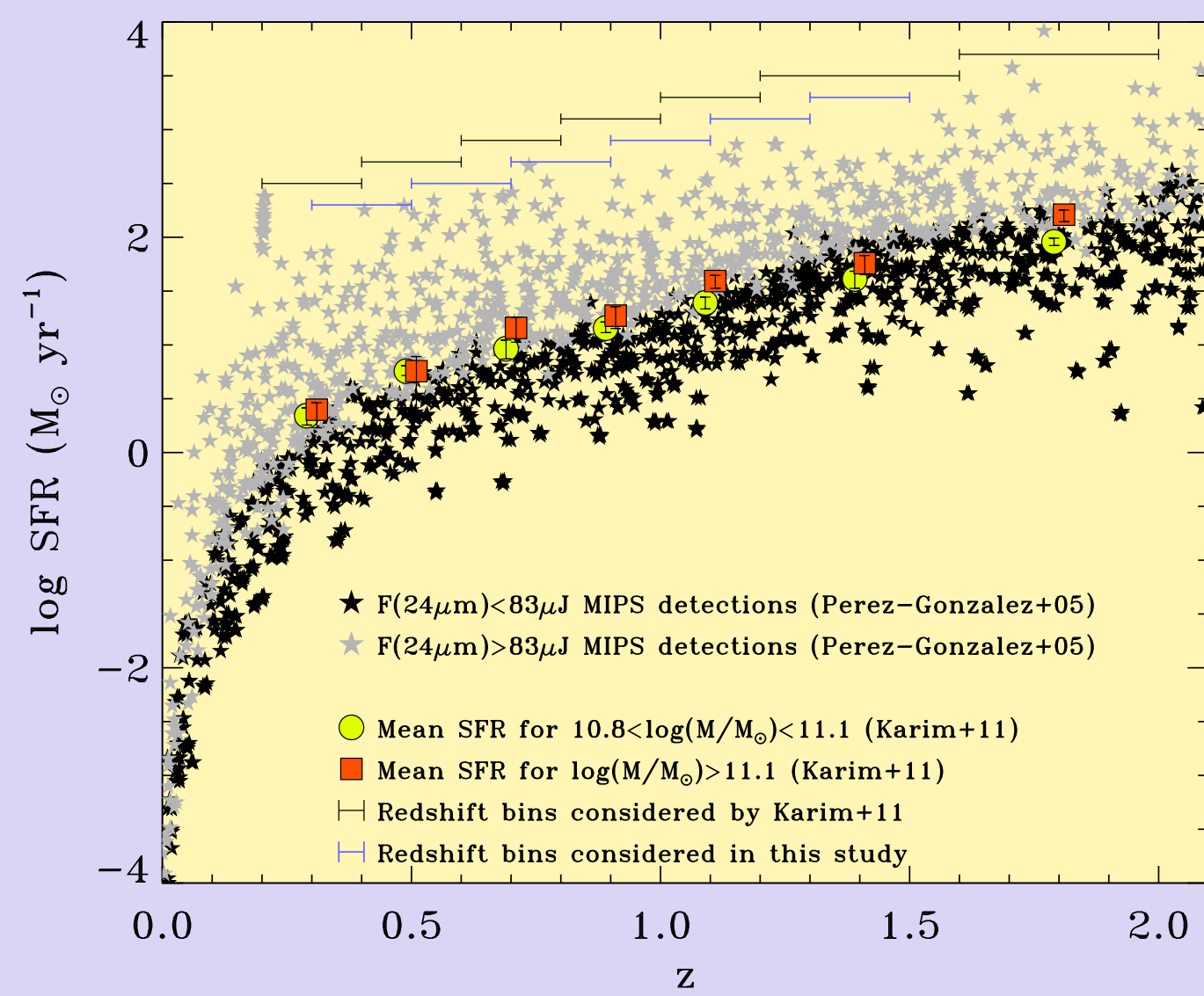


Figura 3.- Red squares: Redshift evolution of the SFR of all galaxies with $\log(M_*/M_\odot) > 11.1$ derived by Karim et al. (2011). Yellow circles: Redshift evolution of the SFR of all galaxies with $10.8 < \log(M_*/M_\odot) < 11.1$ derived by the same authors. Grey stars: Galaxy data from Pérez-González et al. (2005) with $F(24 \mu\text{m}) > 85 \mu\text{J}$. Black stars: Galaxy data from the same authors with $F(24 \mu\text{m}) < 85 \mu\text{J}$. This limiting flux in $24 \mu\text{m}$ naturally isolates galaxies with high (enhanced) SFR compared to the average value of the whole galaxy population at each redshift from those with low SFR, for the mass range considered here.

Table 1. Correspondence between different galaxy evolutionary stages and our red galaxy types.

Galaxy Type	Global morphology	Structural distortion ^a	Star formation ^b
E-S0	Spheroid-dominated	Regular	LSF
Spiral	Disk-dominated	Regular	HSF/LSF
Gas-rich major mergers (merging-nuclei phase)	Disk-dominated	Irregular	HSF/LSF
Gas-rich major mergers (post-merger phase)	Spheroid-dominated	Irregular	HSF/LSF
Gas-poor major mergers	Spheroid-dominated	Irregular	HSF/LSF

^a Non-distorted morphologies are noted as regular, and merger-like distorted ones as irregulars.

^b HSF: objects with enhanced star formation; LSF: objects with star formation lower than the average of the whole galaxy population.

Only major mergers already merged into one body are traced by this study. Galaxy pairs are considered as two still-independent galaxies.

RESULTS

4 Morphological evolution of red galaxies since $z \sim 1.5$

The fraction of red irregular galaxies (major mergers) decreases with cosmic time only relatively to that of regulars, pointing to their transitory nature.

The number density distributions of regular (mostly E-S0's) and of irregulars cross at $z \sim 0.9$ for $M_* > 5 \times 10^{10} M_\odot$.

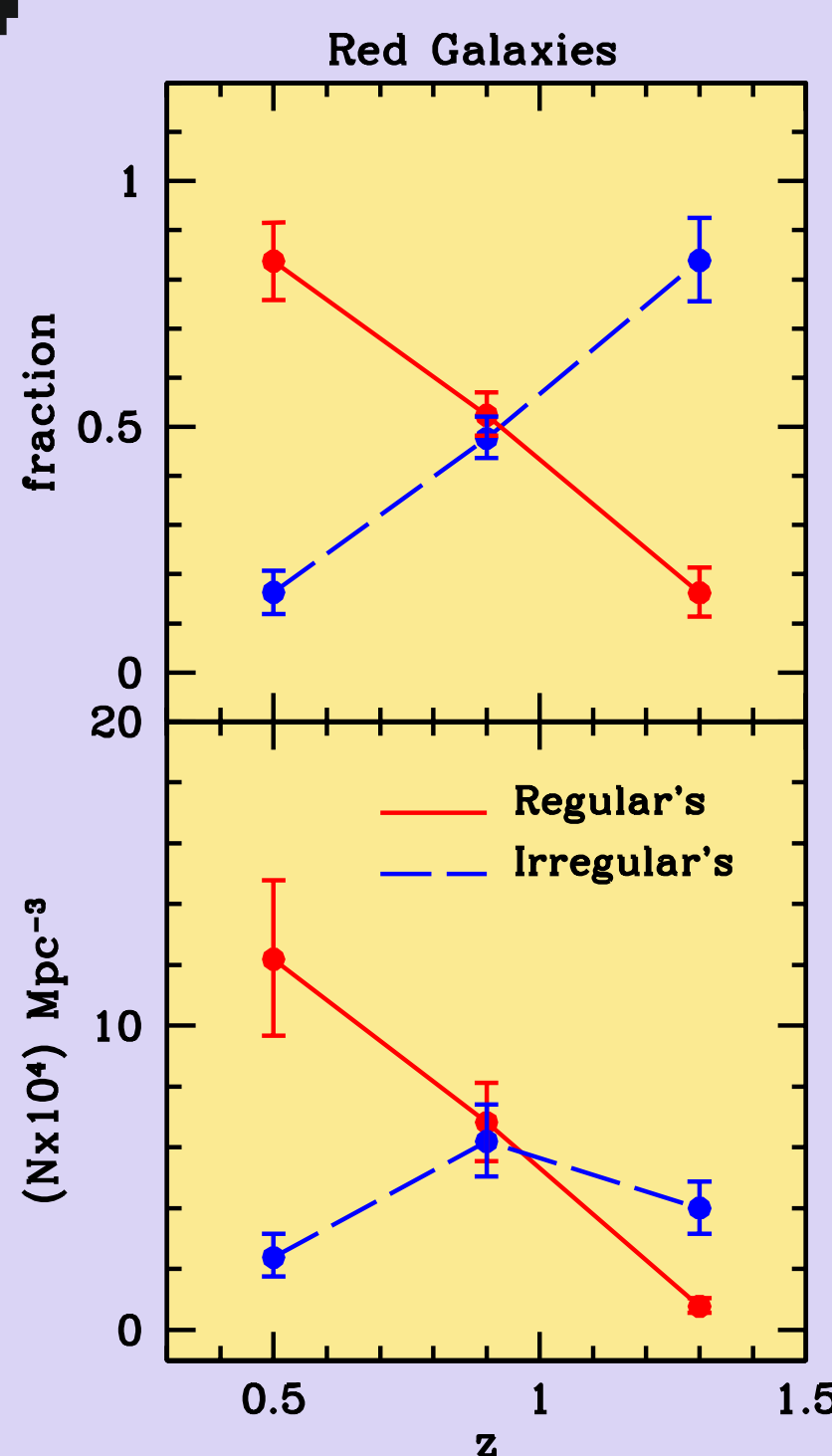


Figura 4.- Top panel: Redshift evolution of the fraction of red massive regular and irregular galaxies (i.e., major mergers) with respect to the total red galaxy population in the three wide redshift bins under consideration ($0.3 < z < 0.7$, $0.7 < z < 1.1$, and $1.1 < z < 1.5$). Bottom panel: Redshift evolution of the number density of regular and irregular massive red galaxies in the same redshift bins.

[The errors in the estimates of the number density are derived considering the following sources of errors: statistical and classification errors, photometric redshift errors, and cosmic variance uncertainties.]

5 Tests to the definitive buildup of massive E-S0's through major mergers

We have performed three observational tests to the data of red galaxies for testing the hierarchical buildup of massive E-S0's, on the base of expectations of the semi-analytical model by Eliche-Moral et al. (2010, EM10 hereafter). They show the existence of a main evolutionary path among red galaxy types at $0.6 < z < 1.2$, being:

Gas-rich major merger \rightarrow Post-merger + Gas-poor major merger \rightarrow Massive E-S0a

Data must fulfill:

Irregular disk \rightarrow irregular spheroid \rightarrow regular spheroid.

This track traces the conversion of blue disks into passive E-S0's through major mergers and dominates the buildup of the Red Sequence at $z > 0.6$.

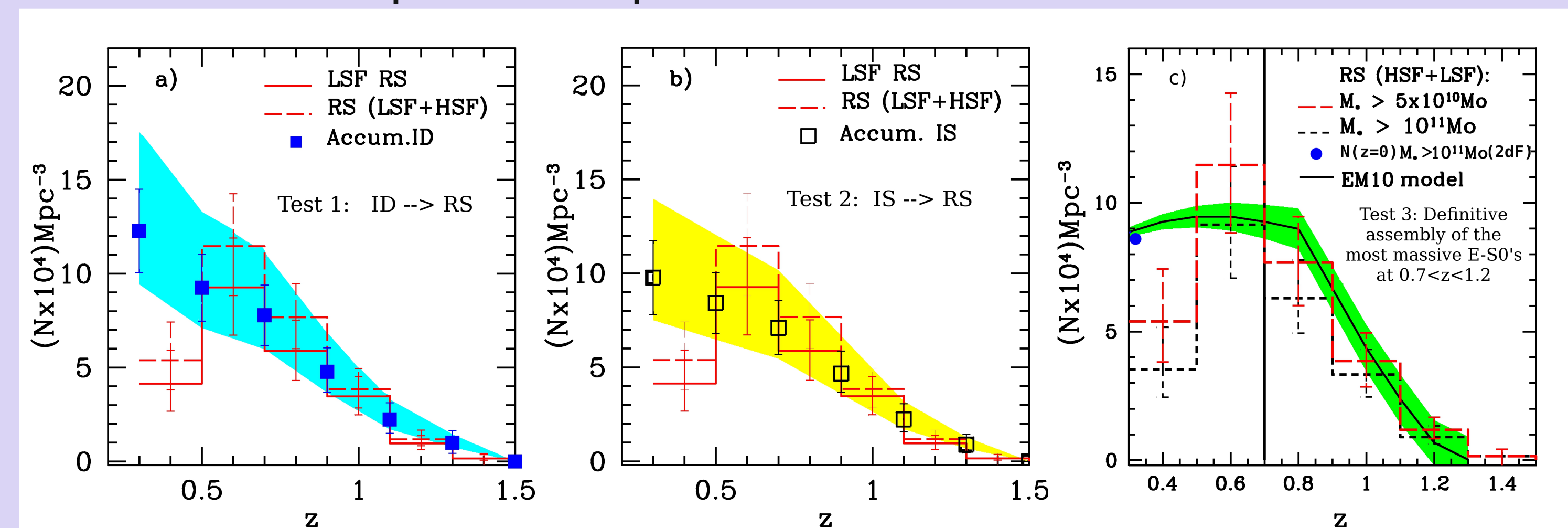


Figura 5.- Panel a) Test 1: Cumulative redshift distribution of red ID's since $z = 1.5$ down to $z = 0.3$, compared to the buildup of massive RS's during the same time period.

Panel b) Test 2: Cumulative redshift distribution of red IS's since $z = 1.5$ down to $z = 0.3$, compared to the buildup of massive RS's during the same time period.

Panel c) Test 3: Comparison of the redshift evolution of the number density of RS's (E-S0's) for two different mass ranges and the predictions of the EM10 model for E-S0's that end up with $M_* > 10^{11} M_\odot$ at $z = 0$. Vertical solid line: Epoch at which the E-S0's with $M_* > 10^{11} M_\odot$ at $z = 0$ can be considered as definitively assembled according to the EM10 model. Blue circle: Local number density of red galaxies with $M_* > 10^{11} M_\odot$ derived by Madgwick et al. (2003) from 2dF survey. The filled areas around the cumulative data points in panels a and b correspond to the uncertainties in the merger detectability timescales, while in panel c indicates the model uncertainties. The lowest redshift bin suffers from incompleteness.

MAIN CONCLUSIONS

We report observational evidence for the first time of the existence of a dominant evolutionary path among massive red galaxies at $0.6 < z < 1.2$, consisting in the conversion of irregular disks into irregular spheroids, and of these ones into regular spheroids.

Results from this study demonstrate that major mergers, despite fulfilling mass-downsizing trends, have played the dominant role in the definitive buildup of present-day E-S0's with $M_* > 10^{11} M_\odot$ at $0.6 < z < 1.2$, in good agreement with the hierarchical scenario proposed in the EM10 model.

References:
Eliche-Moral M. C. et al., 2010, A&A, 519, A55
Karim A. et al., 2011, ApJ, 730, 61
Madgwick D. S. et al., 2003, ApJ, 599, 997
Pérez-González P. G. et al., 2005, ApJ, 630, 82